Diffraction by planar targets of transient focused ultrasonic waves

D. Si Ahmed, H. Djelouah(*)

Faculté de Physique, Université des Sciences et de la Technologie Houari Boumedienne

BP 32, El Alia, Bab-Ezzouar, Algiers, Algeria.

(*) Email: djelouah_hakim@yahoo.fr

Introduction

The impulse response method proposed by Stepanishen [1] has been developed for calculation of the transient field of planar transducers. Later, it has been used by other authors to calculate the impulse field radiated in liquids and solids, for various shapes of plane transducers (disk [2-3], elliptical [4], rectangular [5-6]) and for slightly curved transducers when secondary diffraction phenomenon can be neglected [7-13].

The experimental results of Weight and Hayman [14], Mc Laren [15] and Lhemery [16] shown the resolution in time of the different components of the ultrasonic wave (direct and edge waves) radiated by planar transducers allowing then the validation of the impulse response model. Because of the wave propagation reciprocity, the impulse response method is applicable to the cases of both transmitting and receiving transducers [17-24].

This paper is a contribution to the theoretical and experimental studies of diffraction effects appearing when a small target is placed in the transient ultrasonic field radiated by focused transducers which are often used in non-destructive testing and medicine because focussing improves the sensitivity and the lateral resolution. The impulse response method has been extended in order to take account of the finite size of the targets.

Section I of this paper reviews the impulse response approach used for calculation of the acoustical field radiated by focused transducers. In section II, the theoretical study of the acoustic field radiated by a focused transducer and diffracted by a point like planar target is presented.

In the case of small targets, the detected pressure has been expressed as a convolution in the time domain of the source velocity function with the transmit-receive impulse response. The calculation permitted to prove that for one target, several echoes are observed and they can be interpreted by the direct and edge wave's concept. Section III generalizes this principle to targets of finite size.

In order to verify these simulations experimentally, the focused transducer used is made up of a straight planar transducer coupled to a lens. The waveforms of the signals detected by the transducer are compared to signals which have been calculated using the theoretical model.

Theoretical study of transient ultrasonic focused waves

Case of a transmitting transducer

As described by many authors, the Rayleigh integral constitutes a good approximation for the evaluation of the instantaneous pressure in the classical theory of linear acoustics. At a point M, the pressure $P(M, t)$ radiated in a fluid, by a gently curved focused transducer surrounded by an infinite and rigid baffle, is given by [10-11,13,17]:

$$P(M,t) = \rho \frac{\partial v(t)}{\partial t} * \phi_{iE}(M,t) \quad . \tag{1}$$

ρ is the density of the propagation fluid medium, * is the convolution product in the time domain, $v(t)$ is the normal particle velocity of the source surface, $\phi_{iE}(M, t)$ is called the impulse response in emission for the velocity potential; it represents the velocity potential at the field point M, resulting from an impulsive velocity of all the points belonging to the source [6-7,11,25-27].

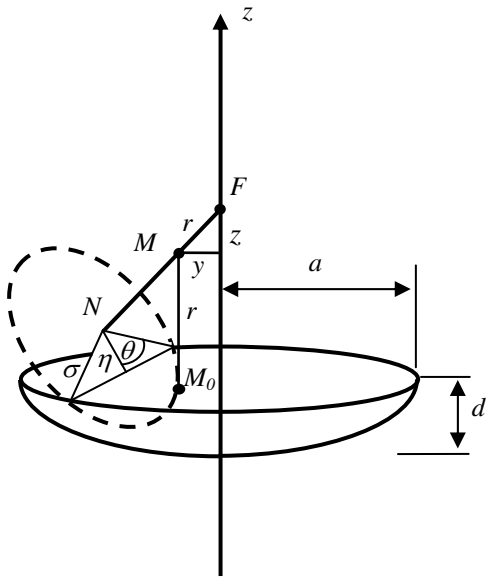

Fig. 1. **Diagram illustrating the geometry and the quantities necessary for the derivation of $\phi_{iE}(M, t)$.**

In this case and if all points of the source vibrate uniformly with the same amplitude, $\phi_{iE}(M, t)$ is given by [11, 13, 17-27]:

$$\phi_{iE}(M,t) = \int_{S_T} \frac{\delta\left(t - \frac{r'}{c}\right)}{2\pi\, r'} dS_T \,, \tag{2}$$

where r' is the distance separating the field point M from the elementary surface dS_T located at the point M_0 belonging to the transducer radiating face, c represents the speed of sound in the fluid.

Table 1. **Expressions of $\phi_{iE}(M, t)$ for different regions**

region I	region II	region III	$\phi_{iE}(M, t)$
$t < t_0$	$t < t_1$	$t < t_1$	0
$t_0 < t < t_1$	$t_1 < t < t_2$		$c\,R / r$
$t_1 < t < t_2$	$t_2 < t < t_0$	$t_1 < t < t_2$	$\frac{c\,\mathrm{R}}{\pi\,\mathrm{r}} \arccos\left(\frac{\eta(t)}{\sigma(t)}\right)$
$t > t_2$	$t > t_0$	$t > t_2$	0

With $\eta(t) = R\left\{\dfrac{\left(1-\frac{d}{R}\right)}{\sin(\alpha)} + \dfrac{\left(\frac{R^2+r^2-c^2t^2}{2rR}\right)}{\tan(\alpha)}\right\}$, $\sigma(t) = R\sqrt{1-\left[\dfrac{R^2+r^2-c^2t^2}{2rR}\right]^2}$, $\alpha = \arctan\left(\dfrac{y}{z}\right)$

r is the distance between the point $M(y, z)$ of the field and the focus F.

Knowing the time function of the source velocity $v(t)$, the derivation of the field pressure $P(M, t)$ requires the knowledge of $\phi_{iE}(M, t)$ which can be easily obtained in the case of a spherical source of radius R, focus F and aperture a.

Because of the symmetry around the z axis, cylindrical co-ordinates are used to locate each point in the field. The z axis coincides with the symmetry axis of the transducer (Fig. 1). The half-space beyond the source is divided into three regions (Fig. 2).

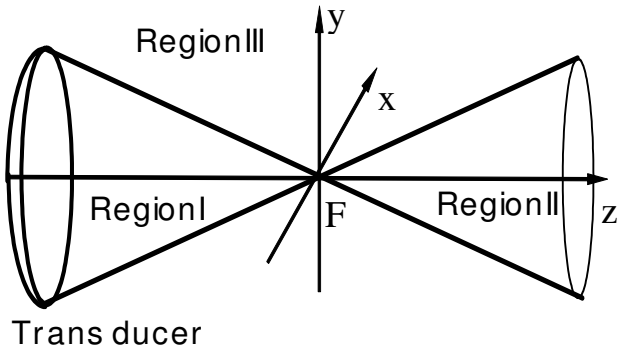

Fig. 2. **The three regions (I, II and III) used to describe the impulse response of a focused source**

Three instants are defined t_0, t_1 and t_2. $t_0 = \dfrac{r_0}{c}$ is the transit time between the field point M and its projection P on the radiating surface that passes through the focus; this instant is not defined in the region III. The instants $t_1 = \dfrac{r_1}{c}$ and $t_2 = \dfrac{r_2}{c}$ are respectively, the propagation time of the vibrations which occur at the point M and issue respectively from the extreme points of the source. The chronology of the arrival times is different in the three regions:

$$\begin{aligned} &\text{region I} \;: t_{min} = t_0 < t_1 < t_2 = t_{max,} \\ &\text{region II} \;: t_{min} = t_1 < t_2 < t_0 = t_{max,} \\ &\text{region III} : t_{min} = t_1 < t_2 = t_{max.} \end{aligned} \qquad (3)$$

The expressions of $\phi_{iE}(M, t)$, as given by Arditi [7], are summarised in Table I.

These results are not valid when the point M is located at the focus. In this later case, the impulse response is given by:

$$\phi_{iE}(M,t) = \mathrm{d}\,\delta\left(t - \frac{R}{c}\right), \qquad (4)$$

where d is the depth of the concave source [10] (Fig. 1), $\delta(\,)$ is the Dirac impulse function.

Case of a receiving transducer

A receiving transducer is sensitive to the acoustic pressure at each point over its surface; the resultant pressure is the average of all these local pressures on the receiver surface.

The average received pressure is given by [11]:

$$\langle P(t)\rangle = \rho\,\frac{\partial\langle\Phi(t)\rangle}{\partial t}, \qquad (5)$$

where $\langle P(t)\rangle$ is the average acoustic potential over the surface of the receiving transducer and it is defined by:

$$\langle\Phi(t)\rangle = \frac{1}{S_T}\int_{S_T}\Phi(M_T,t)\,dS_T \qquad (6)$$

dS_T is an elementary surface located at the point M_T belonging to the source. A flat point target of surface S_c acts as a point source which isotropically (at least towards the transducer) reradiates the pulses incident upon it [14]. The velocity potential at the point M_T belonging to the receiver is expressed by:

$$\phi(M_T,t) = \mathrm{S_c}\,\frac{v\left(t - \frac{OM_T}{c}\right)}{2\pi\,OM_T}, \qquad (7)$$

where S_c is the area of the circular point like source, centre of which is O.

By using the characteristics of the Dirac impulse function, the average acoustic potential over the receiver can be written:

$$\langle\phi(t)\rangle = \frac{S_c}{S_T}\,v_O(t) * \int_{S_T}\frac{\delta\left(t - \frac{OM_T}{c}\right)}{2\pi\,OM_T}\,dS_T, \qquad (8)$$

$$\langle \phi(t) \rangle = \frac{S_c}{S_T}\, v_O(t) * \phi_{\mathrm{iR}}\,(O,t)\,, \qquad (9)$$

$v_O\,(t)$ is the velocity at the point O of the circular target behaving as a secondary source.

$\phi_{\mathrm{iR}}\,(M,\,t)$ is the impulse response in the receiving mode for a source at the point O; it has the same form as the impulse response in the transmitting mode $\phi_{\mathrm{iE}}\,(M,\,t)$. It verifies, therefore, the reciprocity principle [16, 25].

The received pressure can be expressed under this form:

$$\langle P(t) \rangle = \rho \frac{S_c}{S_T} \frac{\partial\, v_0(t)}{\partial t} * \Phi_{\mathrm{iE}}\,(O,t)\,. \qquad (10)$$

Theoretical study of the field diffracted by a point like target and received by a focused transducer

Theory

Here, the transducer is used in the transmitting-receiving mode. The flat target surface is assumed to be perpendicular to the symmetry axis (Oz) of the transducer.

In the assumption of a small point like flat target, with the centre $O(x_{\mathrm{O}},\, y_{\mathrm{O}},\, z_{\mathrm{O}})$, as a rigid point of elementary surface S_c [15], which behaves as a source [16,25], the reflected normal velocity at each point of the target is given by:

$$v(\,M_c\,,\,t) \approx v(O,\,t). \qquad (11)$$

Hereafter, the following notation will be used:

$$v(\,O,\,t) = v_{\mathrm{O}}(\,t\,), \qquad (12)$$

with

$$v_0\,(\,t\,) = -\frac{\partial\, \phi\,(O,t)}{\partial\, z}\,, \qquad (13)$$

where $v_{\mathrm{O}}\,(t)$ is the reflected normal velocity of the target surface, it is opposite to the normal incident velocity, because of the total reflection phenomenon. At the point O, the acoustic potential is expressed by:

$$\phi\,(O,t) = v(t) * \int_{S_T} \frac{\delta\,(t - \dfrac{OM_T}{c})}{2\,\pi\, OM_T}\, dS_T\ . \qquad (14)$$

Then

$$v_0(t) = -\,v(t) * \int_{S_T} \frac{\partial}{\partial\, z} \left(\frac{\delta\,(t - \dfrac{OM_T}{c})}{2\,\pi\, OM_T} \right) dS_T\,, \qquad (15)$$

where M_T is a point of the transmitting transducer, $v(t)$ is the normal velocity of the surface of this transmitting transducer. Then Eq. 15 becomes:

$$v_{\,0}\,(t) = v(t) * \left(\frac{z - z_0}{r\,c} \frac{\partial}{\partial\, \mathrm{t}}\, \phi_{\mathrm{iE}}\,(O,t) + \frac{z\text{-}z_0}{r^2}\, \phi_{\mathrm{iE}}\,(O,t) \right). \qquad (16)$$

In the hypothesis of a nearly punctual target located near the axis:

$$z\text{-}z_{\mathrm{O}} >> x\text{-}x_{\mathrm{O}} \quad \text{and} \quad z\text{-}z_{\mathrm{O}} >> y\text{-}y_{\mathrm{O}}, \qquad (17)$$

so:

$$z\text{-}z_{\mathrm{O}} \sim r \quad \text{and} \quad z\text{-}z_{\mathrm{O}} / r^2 \ \sim\ 1/\ (z\text{-}z_{\mathrm{O}}). \qquad (18)$$

then:

$$v_{\,0}\,(t) = v(t) * \left(\frac{1}{c} \frac{\partial}{\partial\, t}\, \phi_{\mathrm{iE}}\,(O,t) + \frac{1}{z\text{-}z_{\mathrm{O}}}\, \phi_{\mathrm{iE}}\,(O,t) \right). \qquad (19)$$

The second approximation is done concerning expression (19); near the axis, the second term can be neglected because $\dfrac{1}{z\text{-}z_{\mathrm{O}}}\, \phi_{\mathrm{iE}}\,(O,\,t)$ is very small when compared to $\dfrac{1}{c} \dfrac{\partial\, \phi_{\mathrm{iE}}\,(O,\,t)}{\partial\, t}$:

$$v_{\,0}\,(t) \approx \frac{1}{c}\ v(t) * \frac{\partial}{\partial\, t}\, \phi_{\mathrm{iE}}\,(O,t)\ . \qquad (20)$$

Then [18]:

$$v_0\,(\,t\,) = -\frac{\partial\, \phi\,(O,t)}{\partial\, \mathrm{z}} = \frac{P_{inc}\,(O,t)}{\rho\, \mathrm{c}}\,. \qquad (21)$$

After reflection on the flat target, the potential at a point M'_T of the transducer can be written as:

$$\phi\,(M'_T,t) = -\frac{S_c}{\rho\, c}\ P_{inc}(O,t) * \frac{\delta\,(t - \dfrac{OM'_T}{c})}{2\,\pi\, OM'_T} \qquad (22)$$

where P_{inc} is given by Eq. 1.

Then the average resulting pressure is expressed as:

$$\langle P(t) \rangle = \frac{\rho}{S_T} \frac{\partial}{\partial\, t} \int_{S_T} \phi\,(M'_T,t)\, dS'_T\ . \qquad (23)$$

Finally

$$\langle P(t) \rangle = -\frac{\rho}{c} \frac{S_c}{S_T} \frac{\partial v(t)}{\partial t} * \frac{\partial}{\partial t} \left(\phi_{iE}(O,t) * \phi_{iR}(O,t) \right). \qquad (24)$$

By taking into account the characteristics of the convolution and in order to satisfy the reciprocity principle for reception, $\phi_{iR}\,(M,\,t)$ may be replaced by $\phi_{iE}\,(M,\,t)$ [14-15, 25].

The fact that $\phi_{iE}\,(M,\,t)$ appears twice in the form of a self convolution points out the reciprocity existing between radiation and reception [16].

Numerical simulations

Since it constitutes a quite good representation of ultrasonic signals, Finch-Muller's function has been already used [29]. It is used here to describe $v(t)$ (Fig. 3).

$$v(t) = \begin{cases} \sin\left(2\pi\nu t\right) - \dfrac{N}{N+1} \sin\left[\dfrac{N+1}{N} 2\pi\nu t \right] & \text{if} \quad 0 < t < \tau \\ 0 & \text{elsewhere} \end{cases}, \qquad (25)$$

where ν is the frequency, N being the number of cycles in $v\,(\,t\,)$.

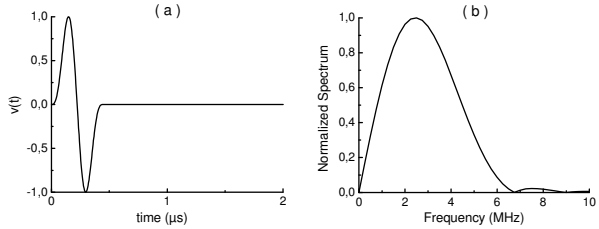

Fig. 3. **a - waveform of $v(t)$ with N=1 and ν=2.25 MHz**; **b - spectrum of $v(t)$**

When the target is on the axis in the region I (Fig. 4.a), the pressure waveform <*P*(*t*)> results from three components, which have the same temporal shape as the source velocity.

These waveforms can be interpreted with the concept of direct wave and edge waves.

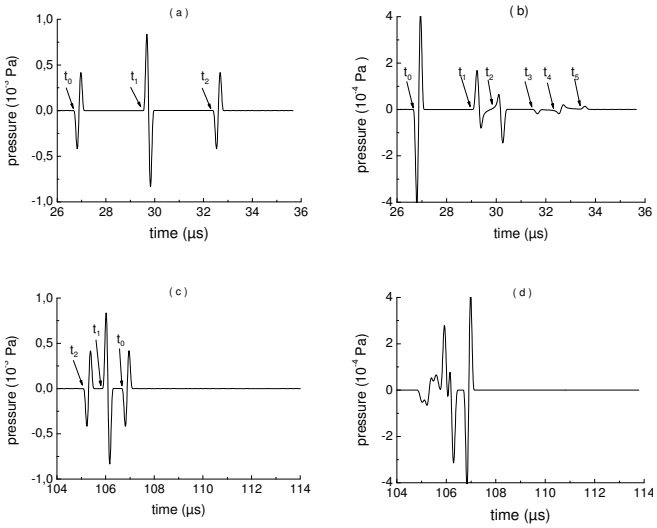

Fig.4. **Time variation of <*P*(*t*)> with *R*=50 mm, a=17.5 mm, ν=2.25 MHz, *N*=1 e=0.04 mm. a) region I (on axis) *z*=-30mm, *y*=0mm.b) region I (off axis) *z*=-30mm, *y*=1mm. c) region II (on axis) *z*=30mm, *y*=0mm. d) region II (off axis) *z*=30mm, *y*=1mm**

The first pulse corresponds to the arrival of the direct wave at the instant $t_0 = \frac{2r_0}{c}$, it represents the direct wave diffracted as a spherical wave by the target and received by the transducer centre, the second pulse corresponds to the simultaneous arrival of two waves at the instant $t_1 = \frac{r_0 + r_1}{c}$; these two pulses correspond respectively to the direct wave diffracted by the target and received by the edge of the transducer and the edge wave emanating from the transducer then diffracted by the target and received by the centre of the transducer. These two pulses produce a pulse of twice amplitude and of opposite sign as compared to the direct wave pulse. The third impulse, which has the same polarity than the first wave, arrives at the instant $t_2 = \frac{2r_1}{c}$; it represents the edge wave emanating from the transducer, diffracted by the target and received by the edge of the transducer. The instants t_0, t_1, t_2 are represented in Fig. 5.

The same observations are noticed when the target is on the axis in the region II, but the arrival times are inverted (Fig. 4.c).

When the target is off-axis in the region I (Fig. 4.b), several pulses are obtained which arrive at different instants. The instant $t_0 = \frac{2r_0}{c}$ corresponds to the arrival of a direct wave which comes from the projection *P* of the target on the source, diffracted by the target and received by the point *P*. The instant $t_1 = \frac{r_0 + r_1}{c}$ corresponds to the simultaneous arrival of two waves, the direct wave emanating from the point *P* then diffracted by the target and finally received by the nearest edge and the edge wave emanating from the nearest edge, diffracted by the target and received by the point *P*. The instant $t_2 = \frac{2r_1}{c}$ represents the arrival of an edge wave emanating from the nearest edge, diffracted by the target and received by the same edge. The instant $t_3 = \frac{r_0 + r_2}{c}$ represents the simultaneous arrival of two pulses: the direct wave emanating from the point *P* diffracted by the target and received by the farthest edge of the source, and the edge wave coming from the farthest edge diffracted by the target and received by the point *P*.

The instant $t_4 = \frac{r_1 + r_2}{c}$ corresponds to the edge wave emanating from the nearest edge diffracted by the target and received by the farthest edge. The instant $t_5 = \frac{2r_2}{c}$ represents the arrival of the edge wave which comes from the farthest edge, diffracted by the target and received by the same edge. The paths corresponding to the instants t_0, t_1, t_2, t_3, t_4 and t_5 are represented in Fig. 6.

In the region II (Fig. 4.d), a similar behaviour can be observed, but with a change in the chronological order of the different contributions.

This interpretation can be extended to the case where the target is located in the region III. In this case, the pressure waveform is composed of three pulses, the first pulse is detected at the instant $t_1 = \frac{2r_1}{c}$; it corresponds to the edge wave emanating from the nearest edge, diffracted by the target and received by the same edge. The instant $t_2 = \frac{r_1 + r_2}{c}$ is the propagation time for a pulse coming from the nearest edge diffracted by the target and then received by the farthest edge. The instant $t_3 = \frac{2r_2}{c}$ is the arrival of the farthest edge wave, diffracted by the target and received by the same edge.

Field diffracted by a target with a finite size and received by an ultrasonic focused transducer

Theory

A rigid flat target of a finite size can be considered as the juxtaposition of several point targets.

It is assumed that, in the transmitting-receiving mode, the transducer is sensitive to the average pressure over its surface.

Then the average pressure received by the transducer can be thought as the sum of the contributions from all elementary point targets that make up its surface [15].

The method for calculation of the resulting pressure consists in dividing the surface of the target into *n* elementary surfaces ΔS_k. For each of these elementary surfaces, the acoustic potential $\Delta\phi_k$ is calculated as previously. At the point M'_T of the transducer, the acoustic potential $\Delta\phi_k$ created by ΔS_k can be written as:

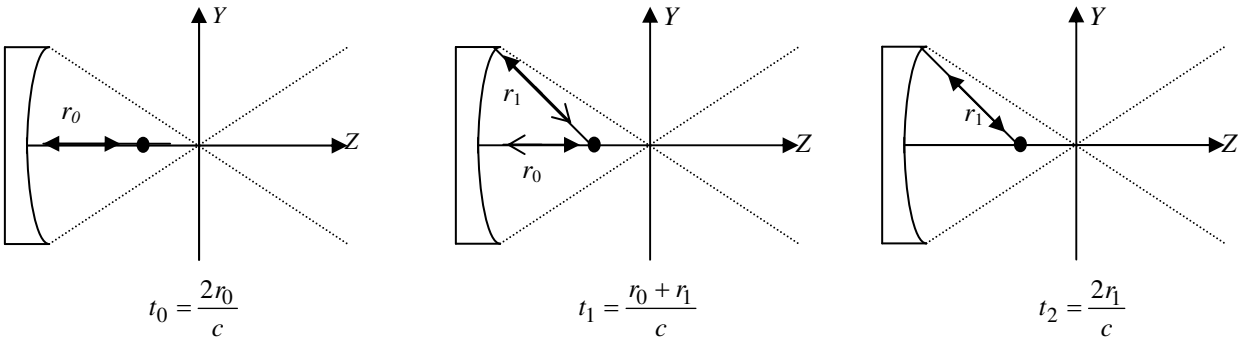

Fig.5. **Representation of the different paths corresponding to instants t_0, t_1, t_2. (target on axis: region I)**

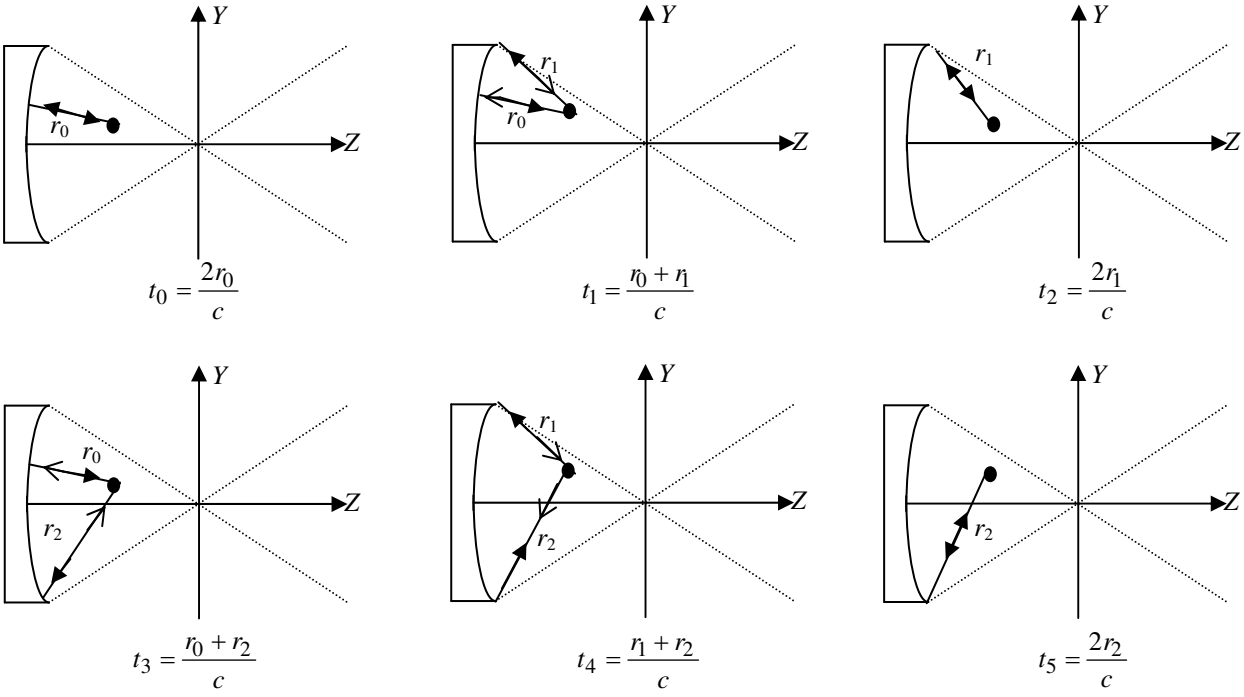

Fig.6. **Representation of different contributions paths corresponding to the instants t_0, t_1, t_2, t_3, t_4, t_5. (target off axis: region I).**

$$\Delta\phi_k\,(M'_T,t) = -\frac{\Delta S_k}{\rho\, c}\; P_{inc}(M_c,t) * \frac{\delta\,(t-\frac{M'_T M_c}{c})}{2\pi\, M'_T M_c}, \quad (26)$$

where $P_{inc}\,(M_c, t)$ is the incident pressure at the point M_c of the target.

Since each elementary surface is considered as a point, the previously used hypotheses are again valuable.

The resulting acoustic potential at the point M'_T of the transducer can be written as:

$$\phi\,(M'_T,t) = \sum_{k=1}^{n} \Delta\,\phi_k\,(M'_T,\mathrm{t}) \quad (27)$$

The received pressure at the point M'_T, is given by:

$$P(M'_T,\mathrm{t}) = -\frac{\rho}{c}\left[\sum_{k=1}^{\mathrm{n}} v(t) * \frac{\partial}{\partial t}\phi_{\mathrm{iE}}\,(M_c,t) * * \frac{\partial}{\partial t}\left(\frac{\delta(t-\frac{M'_T M_c}{c})}{2\pi\, M'_T M_c}\right)\right]\Delta S_k. \quad (28)$$

Fig. 7 shows the geometry for determining the received pressure for a transducer of aperture *a,* and a flat target of the radius *e*.

The source and the flat target are parallel, thus the elementary area ΔS_k can be calculated by:

$$\Delta S_k = r_h\;\theta_h\,(\,r_h\,)\,\Delta\,r_h \quad (29)$$

with:

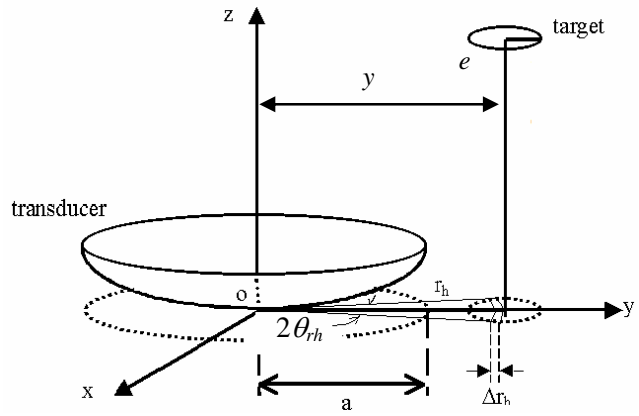

Fig. 7. **Target projection on a plane normal to the transducer axis**

$$r_h = r_1 + (k\text{-}1)\,\Delta r_h, \tag{30}$$

where

$$\Delta r_h = (r_2 - r_1)/N,$$

$$\theta_h(r_h) = \arccos\left(\frac{r_h^2 + y^2 - e^2}{2\,y\,r_h}\right). \tag{31}$$

For an axisymmetric source distribution, $\phi_{\mathrm{iE}}(M, t)$ is independent of the angle $\theta_h(r_h)$ [21], so the pressure at the point M'_T of the receiver is:

$$P(M'_T, t) = -\frac{\rho}{c}\sum_{r_h=r_1}^{r_2} r_h\,\theta_h(r_h)\,\Delta r_h \times$$

$$\times\left[v(t) * \frac{\partial}{\partial t}\phi_{\mathrm{iE}}(M_c, t) * \frac{\partial}{\partial t}\left(\frac{\delta\left(t - \frac{M'_T M_c}{c}\right)}{2\pi\, M'_T M_c}\right)\right], \tag{32}$$

and the average pressure detected by the transducer is:

$$\langle P(t)\rangle = -\frac{\rho}{cS_T}\left[F_1(t) + F_2(t)\right],$$

where

$$F_1(t) = \pi(\Delta r_h)^2\left(\frac{\partial v(t)}{\partial t} * \frac{\partial}{\partial t}(\phi_{\mathrm{iE}}(M_c, t) * (\phi_{\mathrm{iE}}(M_c, t))\right)$$

and

$$F_2(t) = \sum_{r_h=r_1}^{r_2}\left(r_h\,\theta_h(r_h)\,\Delta r_h\right)\times$$

$$\times\left(\frac{\partial v(t)}{\partial t} * \frac{\partial}{\partial t}(\phi_{\mathrm{iE}}(M'_T, t) * (\phi_{\mathrm{iE}}(M'_T, t))\right). \tag{33}$$

Numerical simulations

On the axis, in Region I or Region II, the average pressure is composed of three pulses (Fig. 8a, 8c). The first pulse has the same shape as the velocity waveform of the source, but its amplitude is increased when compared to the case of point like target. On the other hand, the second and the third pulses spread out in the time and their amplitudes decrease.

The effect due to the finite size of the target is more marked on the edge waves because they sweep across the surface of the target. Then, their amplitude decreases. For far positions from the transducer (region II), the target with a finite size behaves as a punctual target.

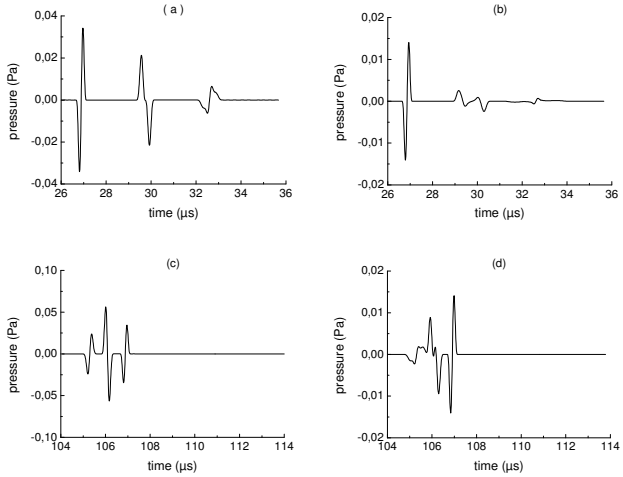

Fig.8. **Variation of <*P*(*t*)> for the target of radius *e*=0.4 mm, with *R*=50mm, *a*=17.5 mm, *ν*=2.25 Mhz and *N*=1: a - target on axis (region I) *z*=-30 mm, *y*=0 mm, b - target off axis (region I) *z*=30mm, *y*=1 mm, c - target on axis (region II) *z*=30 mm, *y*=0mm, d - target off axis (region II) *z*=30 mm, *y*=2 mm**

When the target is off axis (Fig. 8b, 8d), the situation is more complicated. In this location, many pulses are obtained because of the finite size of the target. The pulses corresponding to the edge waves have small amplitudes and are spread out in the time. The amplitude of the first pulse is as much important as the radius of the target is important. Thus it can be concluded that the phenomena of the diffraction are as much apparent as the target radius is small.

A criterion can be defined in order to decide when the target size effect can be neglected. In practice, a target with a finite size can be considered as nearly punctual if the longest time, Δt, required by the incident waves to travel across the target surface is lower than the rise time of $v(t)$ [28]. For satisfying such a condition, the time interval $\Delta t = t_2 - t'_2$ must be smaller than the rise time of $v(t)$, t_2' and t_2 being defined by:

$$t_2 = \frac{2\left[(R\text{-}d + z)^2 + (a + y\text{-}e)^2\right]^{1/2}}{c} \tag{34}$$

$$t'_2 = \frac{\left[(R\text{-}d + z)^2 + (a + y\text{-}e)^2\right]^{1/2}}{c} +$$

$$+ \frac{\left[(R\text{-}d + z)^2 + (a + y + e)^2\right]^{1/2}}{c},$$

where t_2 represents the arrival instant of the leading edge wave and t'_2 is the arrival instant of the last edge wave.

Experimental study

Experimental set up

The experiments were carried out in a tank filled with water. The ultrasonic pressure was measured by using a wide band transducer (nominal frequency ν = 2.25 MHz and diameter D=25.4 mm), coupled to a thin plane-concave lens made of Plexiglas with a curvature radius R_L=30 mm.

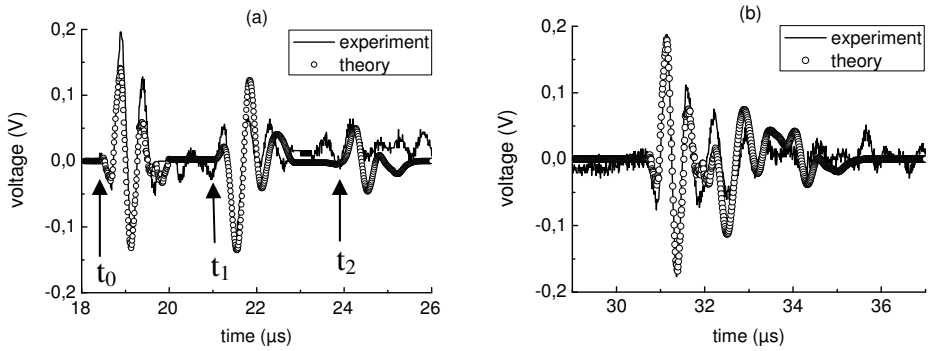

Fig.9. **Ultrasonic signals for a target with a radius *e*=0.5 mm: a - on axis *z* = - 52 mm, *y* = 0 mm, b - off axis *z* = - 43 mm, *y* = 0.5 mm**

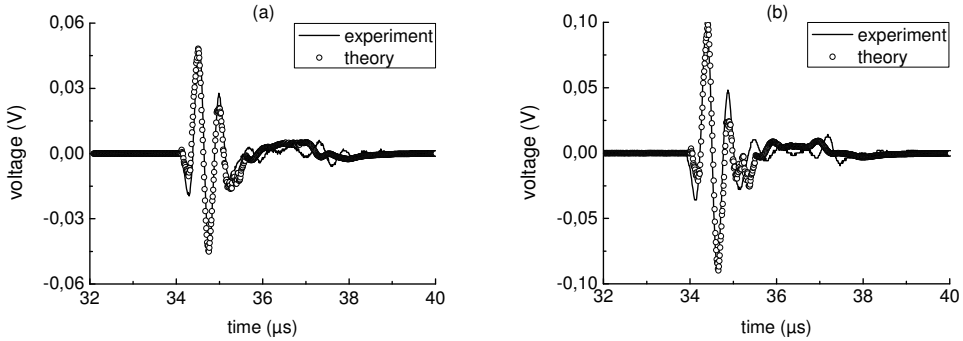

Fig.10. **Ultrasonic signals: a - target with a radius *e* = 2.5 mm, on axis, at *z* = -40 mm, *y* = 0 mm, b - target with a radius *e* = 3.5 mm, on axis, at *z*=-40mm, *y* = 0 mm**

Such a device is equivalent to a spherical focused transducer with a focal length R given by [19, 29]:

$$R = \frac{R_L}{1 - \frac{c}{c_L}}, \tag{35}$$

where c_L is the propagation velocity in the lens. In our case, R=66.4mm.

The transducer is excited by an ultrasonic wide band pulser-receiver. The targets are made of Duralumin, with different radii (0.5 mm, 2.5 mm and 3.5 mm). The target is set perpendicular to the transducer axis and is moved by a mechanical system. The detected signals have been sampled by using a digitizing oscilloscope controlled by a microcomputer.

Method of numeric simulation for experimental results

In the linear case, each element of the electro-acoustic circuit behaves as a linear and invariant system. The voltage signal $s(t)$ observed at the output of the electro-acoustic circuit is:

$$s(t) = < P(t) > * h(t), \tag{36}$$

where $h(t)$ is the impulse response of all the electro-acoustic circuit, the pressure $< P(t) >$ is given by Eq. 32.

It is difficult to evaluate $v(t)$ and $h(t)$ separately. But we show hereafter that we can evaluate the global term $v(t) * h(t)$. In the theoretical study we have verified that, for not too large targets located at the same position on axis in the region I, the first pulse has the same waveform shape and the same spectrum as the source velocity function $v(t)$. Then we can say that this pulse is a pure translation of the velocity waveform $v(t)$, at nearly a multiplier coefficient.

In this situation, we can consider that the average pressure corresponding to the first pulse and detected by the focused transducer can be written as the convolution of the velocity function $v(t)$ and a delayed impulse time function, such as:

$$< P(t) >_{\mathrm{FIRST}} = A\ v(t) *\ \delta(t-t_0), \tag{37}$$

where A is a constant equal to:

$$A = - \frac{\rho S_c}{c S_T}. \tag{38}$$

Experimental results

Fig. 9 and 10 represents the comparison between the experimental signal and the theoretical signal for different target positions on axis and off axis. The previously defined arrival times t_0, t_1 and t_2, are indicated in Fig. 9. A good agreement (shape and duration) can be noticed between the experimental and the calculated waveforms at different points in the field. The measurement points have been arbitrary chosen far from the focus in order to obtain pulses well resolved in time.

Conclusion

The theoretical method described in this paper, allowed an understanding of the diffraction phenomenon, which appears when the acoustic wave radiated by a focused transducer is diffracted by plane targets with different sizes.

The direct and edge waves concept has been used in the interpretation of the diffraction phenomenon. A good agreement has been observed when theoretical signals have been compared with experimental signals. The calculation method can constitute a very interesting mean for predicting complex echo-responses from targets immersed in water and insonified by almost arbitrary transducers.

References

1. **Stepanishen P. R.** Transient radiation from pistons in an infinite planar baffle. J. Acoust. Am. Soc. 1971. Vol.49. No. 5, (part 2). P.1629-1638.
2. **Harris G. R.** Review of transient field theory for a baffled planar piston. J. Acoust. Am. Soc. 1981. Vol.70 (1). P. 10-20.
3. **Weight J. P.** Ultrasonic beam structure in fluid media. J. Acoust. Am. Soc. 1984. Vol.76 (4). P. 1184-1191.
4. **Tjótta J. N., Tjótta S.** Nearfield and farfield of pulsed acoustic radiators. J. Acoust. Am. Soc. 1982. Vol.71. P. 824-834.
5. **San Emeterio J. L., Ullate L.G.** Diffraction impulse response of rectangular transducers. J. Acoust. Am. Soc. 1992. Vol.2. P. 651-662.
6. **Faure P., Cathignol D., Chapelon J.Y.** Diffraction impulse response of arbitrary polygonal plane transducers. Acta acustica. 1994. Vol.2. P.257-263.
7. **Arditi M., Forester F. S., Hunt J.** Transient Field of Concave annular arrays. Ultrasonic Imaging. 1981. No. 3. P. 37-61.
8. **Freedman A.** Sound field of plane or gently curved pulsed radiators. J. Acoust. Am. Soc. 1970. Vol.48. P. 221-227.
9. **Penttinen A., Luukkala M.** The impulse response and pressure nearfield of a curved radiator. J. Phys (D), Appl. phys. 1976. Vol.9. P. 1547-1557.
10. **Fink M. A., Cardoso J. F.** Diffraction Effects in pulse echo measurement. IEEE Transactions of Sonics and Ultrasonics. July 1984. Vol. SU-31. No 4. P. 313-329.
11. **Djelouah H., Baboux J.C., Perdrix M.** Theoretical and experimental study of the field radiated by ultrasonic focused transducers. Ultrasonics. 1991. Vol 29. P. 188-200.
12. **Theumann J.F., Arditi M., Meister J. J., Jacques E.** Acoustic field of concave cylindrical transducers. J. Acoust. Am. Soc. 1990. Vol.88 (2). P. 1160-1169.
13. **Faure P., Catignol D., Chapelon J. Y.** On the pressure field of a transducer in the form of a curved strip. J. Acoust. Am. Soc. 1994. Vol.95 (2). P. 628-637.
14. **Hayman A. J., Weight J. P.** Transmission and reception of short ultrasonic pulses by circular and square transducers. J. Acoust. Am. Soc., Oct 1979. Vol.66 (4). P. 945-951.
15. **Mc Laren S., Weight J. P.** Transient receive mode responses from finite sized targets in fluid media. J. Acoust. Am. Soc. 1987. Vol.82(6). P. 2102-2112.
16. **Lhemery A.** Impulse response method to predict echo-responses from targets of complex geometry. Part I. Theory. J. Acoust. Am. Soc. 1991. Vol.90 (5). P. 2799-2807.
17. **Catignol D., Faure P., Chavrier F.** Acoustic field of plane or spherical transducers. Acta acustica. 1997. Vol. 83. P. 410-418.
18. **Weight J. P, Hayman A. J.** Observations of the propagation of very short ultrasonic pulses and their reflection by small targets. J. Acoust. Soc. Am. 1978. Vol. 63 (2). P. 396-404.
19. **Dernirli R., Saniic J.** Model-based estimation of ultrasonic echoes. Part I: Analysis and algorithms. IEEE Trans. Ultrason. Ferroelectr. Freq. Control. 2001. Vol.48(3). P. 787-802.
20. **Dernirli R., Saniic J.** Model-based estimation of ultrasonic echoes. Part 11: Nondestructive evaluation applications. IEEE Trans. Ultrason. Ferroelectr. Freq. Control. 2001. Vol. 48(3). P. 803-810.
21. **Buiochi F., Martínez O., Gómez-Ullate L., De Espinosa F. M.** A computational method to calculate the transmit-receive mode echo responses from targets of complex geometry. IEEE Ultrasonics symposium. 2004. P. 950-953.
22. **Wilhjelm J. E., Pedersen P. C., Jacobsen S. M.** The influence of roughness, angle, range and transducer type on the echo signal from planar interfaces. IEEE Trans. Ultrason. Ferroelectr. Freq. Control. 2001. Vol.48(2). P. 511-521.
23. **Szabo T. L., Karbeyaz B. U., Cleveland R. O., Miller E. L.** Determining the pulse-echo electromechanical characteristic of a transducer using flat plates and point targets. J. Acoust. Soc. Am. July 2004. Vol.116 (1). P. 90-96.
24. **Mestas J. L. A., Lenz P., Cathignol D.** Determination of the acoustic pressure at and the reflection coefficient of a target through measurements of the absorbed power and the emitter voltage. IEEE Trans. Ultrason. Ferroelectr. Freq. Control. 2004. Vol. 51(1). P. 109-113.
25. **Djelouah H., Baboux J. C., Perdrix M.** The transient field of a planar ultrasonic transducer coupled to a lens: Experiments and simulations. J. Acoust. Soc. Am. 1990. Vol.87 (1). P. 76-80.
26. **Djelouah H., Baboux J. C., Perdrix M.** Experimental determination of the impulse response of axisymmetric focused ultrasonic transducers. J. Phys. D, Appl.phys. 1990. Vol. 23. P. 1135-1142.
27. **Harris G. R.** Transient field of a baffled planar piston having an arbitrary vibration amplitude distribution. J. Acoust. Soc. Am. 1981. Vol.70 (1). P. 186-204.
28. **Ilan A., Weight J. P.** The propagation of short pulses of ultrasound from a circular source coupled to an isotropic solid. J. Acoust. Am. Soc. 1990. Vol.88(2). P. 1142-1151.
29. **Penttinen A., Luukkala M.** Sound pressure near the focal area of an ultrasonic lens. J. Phys (D), Appl. phys. 1976. Vol.9. P. 1927-1936.

D. Si Ahmed, H. Djelouah

Fokusuotųjų ultragarsinių bangų difrakcija naudojant plokščiuosius atspindėtuvus

Reziumė

Teoriškai nagrinėtas fokusuotųjų keitiklių išspinduliuotas ir diskinių plokščiųjų atspindėtuvų išsklaidytas akustinis slėgis skysčiuose. Naudojant mažus atspindėtuvus, nustatytasis slėgis išreiškiamas kaip šaltinio greičio funkcijos laikinė konvoliucija su impulsine siuntimo ir priėmimo charakteristika. Šis rezultatas apibendrintas turint omenyje baigtinio dydžio atspindėtuvus. Taškinio atspindėtuvo atveju yra daug impulsų, kurie gerai atskiriami laike. Apskaičiuotasis slėgio signalas interpretuotas vartojant tiesioginių ir krašto bangų sąvokas. Modeliavimas rodo, kad, naudojant baigtinio dydžio atspindėtuvus, impulsai, atitinkantys krašto bangas, yra mažesnės amplitudės. Taigi difrakcija ir jos efektai labiau reiškiasi kai atspindėtuvas yra mažas. Eksperimentiniame įrenginyje buvo naudojamas 2.25 MHz nominaliojo dažnio ultragarsinis plokščiasis keitiklis su fokusuojančiuoju lęšiu. Skirtingo skersmens cilindriniai strypai buvo naudojami kaip atspindėtuvai. Eksperimentiniai rezultatai gerai atitiko teorinį modelį.

Pateikta spaudai 2005 10 25